

# Hepatology Journal

Copy of e-mail Notification

Your article (11-0959.24701) from Hepatology is available for download.

Hepatology Published by John Wiley & Sons, Inc.

Dear Author,

Your article page proofs for Hepatology are ready for review. John Wiley & Sons has made this article available to you online for faster, more efficient editing. Please follow the instructions below and you will be able to access a PDF version of your article as well as relevant accompanying paperwork.

First, make sure you have a copy of Adobe Acrobat Reader software to read these files. This is free software and is available for user downloading at <http://www.adobe.com/products/acrobat/readstep.html>.

Open your web browser, and enter the following web address:

<http://115.111.50.156/jw/retrieval.aspx>

You will be prompted to log in, and asked for a password. Your login name will be your email address, and your password will be c69f857c5e4f

Example:

Login: your e-mail address

Password: c69f857c5e4f

The site contains one file, containing:

- Author Instructions Checklist
- Adobe Acrobat Users - NOTES tool sheet
- Reprint Order Information
- A copy of your page proofs for your article

Read your page proofs carefully and:

- indicate changes or corrections in the margin of the page proofs or via Adobe Notes
- answer all queries (footnotes A,B,C, etc.) on the last page of the PDF proof
- proofread any tables and equations carefully
- check your figure legends for accuracy

Within 48 hours, please return via e-mail or fax all materials to the address given below. This will include:

Page proofs with corrections

# Hepatology Journal

Copy of e-mail Notification

Return to:

Hepatology Production

E-mail: [hepjournal@wiley.com](mailto:hepjournal@wiley.com)

John Wiley & Sons, Inc.

111 River Street, Mail Stop 8-02

Hoboken, NJ 07030

TEL: (201) 748-5762

FAX: (201) 748-6281/6182

Technical problems? If you experience technical problems downloading your file or any other problem with the website listed above, please contact Teresa Beard (e-mail: [beardt@cadmus.com](mailto:beardt@cadmus.com)).

Questions regarding your article? Please don't hesitate to contact me with any questions about the article itself, or if you have trouble interpreting any of the questions listed at the end of your file. **REMEMBER TO INCLUDE YOUR ARTICLE NO. (11-0959.24701) WITH ALL CORRESPONDENCE.** This will help both of us address your query most efficiently.

As this e-proofing system was designed to make the publishing process easier for everyone, we welcome any and all feedback. Thanks for participating in our e-proofing system!

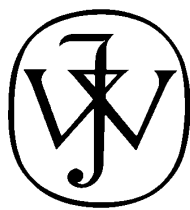
This e-proof is to be used only for the purpose of returning corrections to the publisher.

Sincerely,

Paula Vetrovec

Hepatology Production

E-mail: [hepjournal@wiley.com](mailto:hepjournal@wiley.com)



# WILEY

*Publishers Since 1807*

111 RIVER STREET, HOBOKEN, NJ 07030

## HEPATOLOGY PRODUCTION

**\*\*\*IMMEDIATE RESPONSE REQUIRED\*\*\***

Please follow these instructions to avoid delay of publication.

**READ PROOFS CAREFULLY**

- This will be your only chance to review these proofs. **Please note that once your corrected article is posted online, it is considered legally published, and cannot be removed from the Web site for further corrections.**
- Please note that the volume and page numbers shown on the proofs are for position only.

**ANSWER ALL QUERIES ON PROOFS** (Queries for you to answer are attached as the last page of your proof.)

- Mark all corrections directly on the proofs. Note that excessive author alterations may ultimately result in delay of publication and extra costs may be charged to you.

**CHECK FIGURES AND TABLES CAREFULLY**

- Check size, numbering, and orientation of figures.
- All images in the PDF are downsampled (reduced to lower resolution and file size) to facilitate Internet delivery. These images will appear at higher resolution and sharpness in the printed article.
- Review figure legends to ensure that they are complete.
- Check all tables. Review layout, title, and footnotes.

RETURN  PROOFS

**PLEASE RETURN PROOFS (VIA FAX, E-MAIL, OR OVERNIGHT COURIER) WITHIN 48 HOURS OF RECEIPT TO:**

QUESTIONS?

**Paula Vetovec**, Associate Production Manager  
**Hepatology Production**  
**E-mail: [hepjournal@wiley.com](mailto:hepjournal@wiley.com)**  
**FAX: 201-748-6281/6182**

John Wiley & Sons, Inc.  
111 River St., Mail Stop 8-02  
Hoboken, NJ 07030  
Phone: 201-748-5762

Refer to journal acronym and article production number  
(i.e., HEP 00-0001.20000 for HEPATOLOGY ms 00-0001.20000).

## Softproofing for advanced Adobe Acrobat Users – NOTES tool

NOTE: ADOBE READER FROM THE INTERNET DOES NOT CONTAIN THE NOTES TOOL USED IN THIS PROCEDURE.

Acrobat annotation tools can be very useful for indicating changes to the PDF proof of your article. By using Acrobat annotation tools, a full digital pathway can be maintained for your page proofs.

The NOTES annotation tool can be used with either Adobe Acrobat 6.0 or Adobe Acrobat 7.0. Other annotation tools are also available in Acrobat 6.0, but this instruction sheet will concentrate on how to use the NOTES tool. Acrobat Reader, the free Internet download software from Adobe, DOES NOT contain the NOTES tool. In order to softproof using the NOTES tool you must have the full software suite Adobe Acrobat Exchange 6.0 or Adobe Acrobat 7.0 installed on your computer.

### Steps for Softproofing using Adobe Acrobat NOTES tool:

1. Open the PDF page proof of your article using either Adobe Acrobat Exchange 6.0 or Adobe Acrobat 7.0. Proof your article on-screen or print a copy for markup of changes.
2. Go to Edit/Preferences/Commenting (in Acrobat 6.0) or Edit/Preferences/Commenting (in Acrobat 7.0) check “Always use login name for author name” option. Also, set the font size at 9 or 10 point.
3. When you have decided on the corrections to your article, select the NOTES tool from the Acrobat toolbox (Acrobat 6.0) and click to display note text to be changed, or Comments/Add Note (in Acrobat 7.0).
4. Enter your corrections into the NOTES text box window. Be sure to clearly indicate where the correction is to be placed and what text it will effect. If necessary to avoid confusion, you can use your TEXT SELECTION tool to copy the text to be corrected and paste it into the NOTES text box window. At this point, you can type the corrections directly into the NOTES text box window. **DO NOT correct the text by typing directly on the PDF page.**
5. Go through your entire article using the NOTES tool as described in Step 4.
6. When you have completed the corrections to your article, go to Document/Export Comments (in Acrobat 6.0) or Comments/Export Comments (in Acrobat 7.0). Save your NOTES file to a place on your harddrive where you can easily locate it. **Name your NOTES file with the article number assigned to your article in the original softproofing e-mail message.**
7. **When closing your article PDF be sure NOT to save changes to original file.**
8. To make changes to a NOTES file you have exported, simply re-open the original PDF proof file, go to Document/Import Comments and import the NOTES file you saved. Make changes and reexport NOTES file keeping the same file name.
9. When complete, attach your NOTES file to a reply e-mail message. Be sure to include your name, the date, and the title of the journal your article will be printed in.



### **Additional reprint purchases**

Should you wish to purchase additional copies of your article, please click on the link and follow the instructions provided:

<https://caesar.sheridan.com/reprints/redirect.php?pub=10089&acro=HEP>

Corresponding authors are invited to inform their co-authors of the reprint options available.

Please note that regardless of the form in which they are acquired, reprints should not be resold, nor further disseminated in electronic form, nor deployed in part or in whole in any marketing, promotional or educational contexts without authorization from Wiley. Permissions requests should be directed to mail to: [permissionsus@wiley.com](mailto:permissionsus@wiley.com)

For information about 'Pay-Per-View and Article Select' click on the following link: [wileyonlinelibrary.com/aboutus/ppv-articleselect.html](http://wileyonlinelibrary.com/aboutus/ppv-articleselect.html)

# Osteopontin, an Oxidant Stress-Sensitive Cytokine, Up-regulates Collagen I via Integrin $\alpha_v\beta_3$ Engagement and Phosphoinositide 3-Kinase/ Phosphorylated Akt/Nuclear Factor Kappa Light-Chain Enhancer of Activated B Cells Signaling

Raquel Urtasun,<sup>1\*</sup> Aritz Lopategi,<sup>1\*</sup> Joseph George,<sup>1</sup> Tung-Ming Leung,<sup>1</sup> Yongke Lu,<sup>1</sup> Xiaodong Wang,<sup>1</sup> Xiaodong Ge,<sup>1</sup> Maria Isabel Fiel,<sup>2</sup> and Natalia Nieto<sup>1</sup>

A key feature in the pathogenesis of liver fibrosis is fibrillar collagen I deposition; yet, mediators that could be key therapeutic targets remain elusive. We hypothesized that osteopontin (OPN), an extracellular matrix (ECM) cytokine expressed in hepatic stellate cells (HSC), could drive fibrogenesis by modulating the HSC profibrogenic phenotype and collagen I expression. Recombinant OPN (rOPN) up-regulated collagen I protein in primary HSCs in a transforming growth factor beta-independent fashion, whereas it down-regulated matrix metalloprotease-13, thus favoring scarring. rOPN activated primary HSC—confirmed by increased  $\alpha$ -smooth muscle actin expression—and enhanced their invasive and wound-healing potential. HSCs isolated from wild-type (WT) mice were more profibrogenic than those from OPN knockout (*Opn*<sup>-/-</sup>) mice and infection of primary HSCs with an Ad-OPN-increased collagen I, indicating correlation between both proteins. OPN induction of collagen I occurred via integrin  $\alpha_v\beta_3$  engagement and activation of the phosphoinositide 3-kinase/ phosphorylated Akt/nuclear factor kappa light-chain enhancer of activated B cells (PI3K/pAkt/NF $\kappa$ B)—signaling pathway, whereas cluster of differentiation 44 binding and mammalian target of rapamycin/70-kDa ribosomal protein S6 kinase were not involved. Neutralization of integrin  $\alpha_v\beta_3$  prevented the OPN-mediated activation of the PI3K/pAkt/NF $\kappa$ B—signaling cascade and collagen I up-regulation. Likewise, inhibition of PI3K and NF $\kappa$ B blocked OPN-mediated collagen I increase. Hepatitis C Virus cirrhotic patients showed coinduction of collagen I and cleaved OPN, compared to healthy individuals. Acute and chronic liver injury by CCl<sub>4</sub> injection or thioacetamide (TAA) treatment elevated OPN expression. Reactive oxygen species up-regulated OPN *in vitro* and *in vivo*, and antioxidants prevented this effect. Transgenic mice overexpressing OPN in hepatocytes (*Opn*<sup>HEP</sup> Tg) mice developed spontaneous liver fibrosis, compared to WT mice. Last, chronic CCl<sub>4</sub> injection and TAA treatment caused more liver fibrosis to WT than to *Opn*<sup>-/-</sup> mice, and the reverse occurred in *Opn*<sup>HEP</sup> Tg mice. **Conclusion:** OPN emerges as a cytokine within the ECM protein network driving the increase in collagen I protein, contributing to scarring and liver fibrosis. (HEPATOLOGY 2011;00:000-000)

Fibrogenesis, or activation of the wound-healing response to persistent liver injury, is characterized by changes in the composition and quantity of extracellular matrix (ECM) deposits distorting the normal hepatic architecture by forming fibrotic scars. Failure to degrade accumulated ECM is a major reason why fibrosis progresses to cirrhosis. Emerging antifibrogenic therapies aim at inhibiting the activation

Abbreviations: p70S6K, 70-kDa ribosomal protein S6 kinase; Abs, antibodies; ALT, alanine aminotransferase; BSO, L-buthionine sulfoximine; CD, cluster of differentiation; CYP2E1, cytochrome P450 2E1; ECM, extracellular matrix; EE, ethyl ester; GSH, glutathione; HCV, hepatitis C virus; H&E, hematoxylin and eosin; HSCs, hepatic stellate cells; IgG, immunoglobulin G; IHC, immunohistochemical; IKK, I kappa B kinase; MMP, matrix metalloprotease; MO, mineral oil; NF $\kappa$ B, nuclear factor kappa light-chain enhancer of activated B cells; NOS2, type 2 nitric oxide synthase; OPN, osteopontin; *Opn*<sup>-/-</sup>, osteopontin knockout mice; *Opn*<sup>HEP</sup> Tg, transgenic mice overexpressing OPN in hepatocytes; pAkt, phosphorylated Akt; PDTC, pyrrolidine dithiocarbamate; pERK, phosphorylated extracellular signal-related kinase; PI3K, phosphoinositide 3-kinase; rOPN, recombinant OPN; pp38, phosphorylated p38; SAM, S-adenosylmethionine; SEM, standard error of the mean;  $\alpha$ -SMA,  $\alpha$ -smooth muscle actin; TAA, thioacetamide; TGF- $\beta$ , transforming growth factor beta; WT, wild type.

of profibrogenic cells to prevent fibrillar collagen I deposition, degrading excessive ECM to recover normal liver architecture, and restoring functional liver mass.

Although different cell types contribute to the increase in fibrillar collagen I during hepatic fibrogenesis, they all undergo a common process of differentiation and acquisition of a classical myofibroblast-like phenotype. Hepatic stellate cells (HSCs) are considered a central ECM-producing cell within the injured liver,<sup>1</sup> playing a significant role in collagen I deposition when hepatocellular injury is concentrated within the liver lobule and sinusoids. In the healthy liver, they reside in the sinusoidal space of Disse; however, during chronic injury, they activate while acquiring motile, proinflammatory, and profibrogenic properties.<sup>2</sup> Activated HSCs migrate and accumulate at the sites of tissue repair, secreting large amounts of ECM, mostly collagen I, and regulating ECM remodeling. Up-regulation of fibrillar collagen I is thus a key event leading to scarring, the pathophysiological hallmark of liver fibrosis.

Though some current therapies have proven beneficial, dissecting key profibrogenic mechanisms, pathways, and mediators of disease progression is vital. Several studies have identified osteopontin (OPN) as significantly up-regulated during liver injury and in HSCs.<sup>3-6</sup> OPN is a soluble cytokine and a matrix-bound protein that can remain intracellular or is secreted, hence allowing autocrine and paracrine signaling.<sup>7,8</sup> OPN, as a matricellular phosphoglycoprotein, functions as an adaptor and modulator of cell-matrix interactions.<sup>8</sup> Among its many roles, it regulates cell migration, ECM invasion, and cell adhesion resulting from its ability to bind integrins—through its RGD motif, or cluster of differentiation (CD)44, by a cryptic site (SVVYGLR)—exposed after cleavage by thrombin, plasminogen, plasmin, cathepsin B, and some matrix metalloproteinases (MMPs).<sup>5,9</sup> OPN

expression increases in tumorigenesis, angiogenesis, and, in response to inflammation, cellular stress and injury.<sup>10-14</sup> OPN plays an important role in regulating tissue remodeling and cell survival as well as in chemo-attracting inflammatory cells.<sup>15</sup> Moreover, osteopontin knockout (*Opn*<sup>-/-</sup>) mice show matrix disarrangement and alteration of collagen fibrillogenesis in cartilage, compared to their wild-type (WT) littermates.<sup>16</sup>

There is limited information on the contribution of OPN to HSC profibrogenic behavior and the molecular mechanisms and signaling pathways involved in governing collagen I protein expression during the fibrogenic response to liver injury.<sup>3-6,17</sup> Because OPN is expressed in HSCs,<sup>3-6</sup> we hypothesized that OPN could trigger signals capable of up-regulating collagen I *per se*, hence acting as a feed-forward mechanism promoting scarring. Therefore, the major aim of this work was to determine how OPN could become a profibrogenic “switch” and to characterize the underlying cellular mechanism for this effect. In the present study, we identified a role for intracellular OPN in increasing collagen I, the HSC membrane proteins engaged by extracellular OPN, the proximal signaling molecules/stress-sensitive kinases activated upon binding that trigger the profibrogenic cascade, the ability of OPN to respond to oxidant stress, and the effect of *Opn* ablation or overexpression on collagen I deposition *in vivo*.

## Materials and Methods

Please see Supporting Materials for a detailed description of experimental procedures.

## Results

**Recombinant OPN Slightly Increases HSC Proliferation Rates and Promotes HSC Migration.** Recombinant OPN (rOPN) did not alter HSC viability, but slightly induced proliferation rates, both in rat and

---

From the Division of Liver Diseases, Departments of<sup>1</sup>Medicine and<sup>2</sup>Division of Liver Diseases, Departments of Pathology, Mount Sinai School of Medicine, New York, NY.

Received May 23, 2011; accepted September 14, 2011.

This work was supported by postdoctoral fellowships from the Government of Navarre (Spain) (to R.U.) and from the Basque Government (Spain) (to A.L.), U.S. Public Health Service Grants 5R01 DK069286 and 2R56 DK069286 from the National Institute of Diabetes and Digestive and Kidney Diseases, and 5P20 AA017067 from the National Institute on Alcohol Abuse and Alcoholism (to N.N.).

\*These authors made an equal contribution to this work.

Address reprint requests to: Natalia Nieto, Pharm.D., M.Sc., Ph.D., Division of Liver Diseases, Department of Medicine, Mount Sinai School of Medicine, Box 1123, 1425 Madison Avenue, Room 11-70, New York, NY 10029. E-mail: natalia.nieto@mssm.edu; fax: +1 (212) 849-2574.

Copyright © 2011 by the American Association for the Study of Liver Diseases.

View this article online at [wileyonlinelibrary.com](http://wileyonlinelibrary.com).

DOI 10.1002/hep.24701

Potential conflict of interest: Nothing to report.

Additional Supporting Information may be found in the online version of this article.

AQ3

AQ4

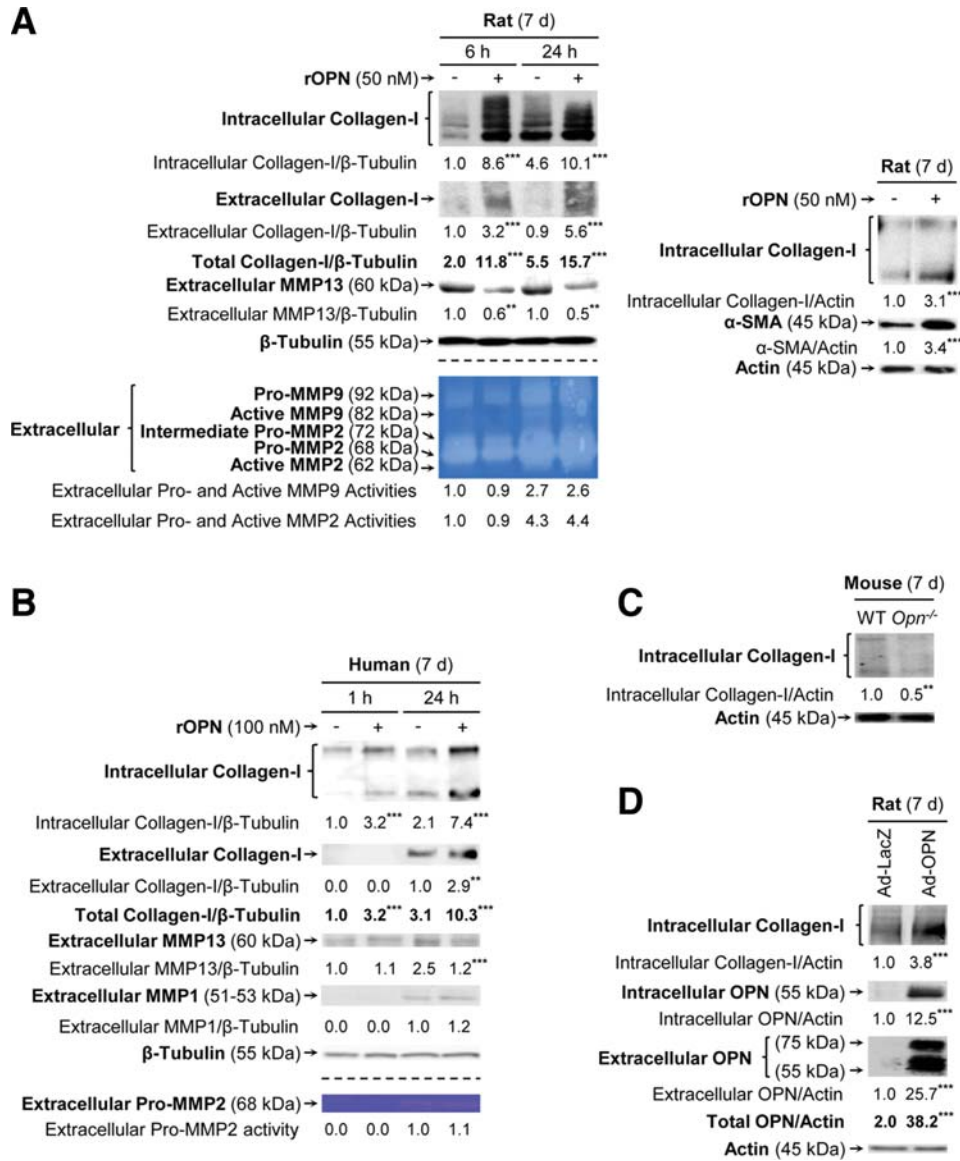


Fig. 1. Profibrogenic effects of rOPN in primary HSCs. Primary rat HSCs cultured for 7 days were treated with 0-50 nM of rOPN for 6 and 24 hours. Western blotting analysis of intra- and extracellular collagen I, extracellular MMP-13, and β-tubulin. Gelatine zymography showing extracellular pro-, intermediate, and active MMP-2 and -9 (A, left). Western blotting analysis of intracellular collagen I, α-SMA, and actin in rat HSCs treated with 0-50 nM of rOPN for 24 hours (A, right). Human HSCs cultured for 7 days were treated with 0-100 nM of rOPN for 1 and 24 hours. Western blotting analysis of intra- and extracellular collagen I, extracellular MMP-13 and -1, and β-tubulin. Pro-MMP2 activity was measured by gelatine zymography. Extracellular MMP-9 activity was undetectable (not shown) (B). Western blotting analysis of intracellular collagen I and actin in HSCs from WT and *Opn*<sup>-/-</sup> mice. Extracellular collagen I was undetectable (C). Western blotting analysis of intracellular collagen I and OPN, as well as extracellular OPN in rat HSCs infected with Ad-LacZ or with Ad-OPN for 48 hours. Extracellular collagen I was undetectable (D). Results are expressed as average values. Experiments were performed in triplicates four times. \*\**P* < 0.01 and \*\*\**P* < 0.001 for rOPN, *Opn*<sup>-/-</sup>, and Ad-OPN versus control, WT, and Ad-LacZ, respectively.

in human HSCs (Supporting Fig. 1); however, rOPN caused a 2-fold increase in the invasive potential or chemotaxis (Supporting Fig. 2A,B) and enhanced the wound-closure ability of rat HSCs (Supporting Fig. 2C), important functions gained by HSC during their activation that contribute to their profibrogenic ability. Neutralizing antibodies (Abs) to α<sub>v</sub>β<sub>3</sub> integrin and OPN blocked the effects on HSC invasion (not shown) and on closure ability (Supporting Fig. 2C).

**rOPN Induces Profibrogenic Effects in Primary HSCs.** Upon stimulation with rOPN, rat HSCs up-regulated intra- and extracellular collagen I in a time-dependent fashion (Fig. 1A, left). Denatured rOPN did not elevate collagen I, thus confirming the specificity of rOPN effect on collagen I in HSCs (not shown). rOPN lowered extracellular MMP-13 protein by 50%, contributing to extracellular collagen I accumulation. Reciprocal modulation of MMP-13 and collagen I has

F1

COLOR

been previously described in rat HSCs.<sup>18</sup> Extracellular pro-, intermediate, and active MMP-2 and -9 remained unchanged (Fig. 1A, left). Likewise, tissue inhibitor of MMP1 was comparable (not shown). rOPN induced rat HSC activation, as shown by the increase in collagen I and alpha smooth muscle actin ( $\alpha$ -SMA) proteins (Fig. 1A, right). Analogous results were observed in human HSC (Fig. 1B).

Because of the ability of HSC to secrete transforming growth factor beta (TGF- $\beta$ ),<sup>19</sup> along with its well-known profibrogenic effect,<sup>20</sup> rat HSCs were treated with anti-TGF- $\beta$  Ab. Neutralization of TGF- $\beta$  did not alter the rOPN-mediated induction of collagen I, thus implying a mechanism independent of TGF- $\beta$  production by HSCs (Supporting Fig. 3).

To dissect whether intracellular OPN could play an autocrine role in modulating collagen I expression, HSCs were isolated from WT and *Opn*<sup>-/-</sup> mice. WT HSCs appeared more profibrogenic than *Opn*<sup>-/-</sup> HSCs, because intracellular collagen I expression at 7 days of culture was higher in WT HSCs than in *Opn*<sup>-/-</sup> HSCs (Fig. 1C). Infection of rat HSCs with an Ad-OPN increased intracellular collagen I and intra- and extracellular OPN, compared to HSCs infected with Ad-LacZ (Fig. 1D). Therefore, a novel autocrine role for intracellular OPN in modulating collagen I deposition was identified.

**Anti- $\alpha_v\beta_3$  Integrin Ab Blocks the rOPN-Driven Collagen I Increase.** Because OPN is also a soluble cytokine and a matrix-bound protein, we next evaluated the role of extracellular OPN-mediated signaling (i.e., paracrine role) on collagen I induction in HSCs. OPN signals by integrins—mostly integrin  $\alpha_v\beta_3$  highly expressed in HSCs<sup>21-23</sup>—and via CD44, also expressed in HSCs.<sup>24</sup> Incubation with anti- $\alpha_v\beta_3$  integrin blocked rOPN-driven total collagen I (intra- plus extracellular) increase in rat HSCs, whereas no major effect was observed by anti-CD44 (Fig. 2A). Neutralization of other integrins (i.e.,  $\beta_1$ ,  $\beta_5$ , and  $\beta_6$ ) failed to prevent the increase in collagen I by rOPN (not shown). Similar results were observed in human HSCs (not shown).

**rOPN Increases Collagen I Protein by Activation of the PI3K/pAkt/NF $\kappa$ B-Signaling Pathway.** Given that collagen I protein is highly responsive to oxidant stress-sensitive kinases, we analyzed the expression of protein kinases involved in regulating collagen I expression, such as phosphorylated p38 (pp38),<sup>25,26</sup> phosphorylated extracellular signal-related kinase (pERK1/2),<sup>27</sup> pJNK,<sup>28,29</sup> phosphoinositide 3-kinase (PI3K), and phosphorylated Akt (pAkt).<sup>26,30</sup> Only PI3K and the ratio of pAkt<sup>473</sup>Ser/Akt were elevated time dependently by rOPN up to 3 hours in rat HSC

(Fig. 2B) and up to 1 hour in human HSCs (Supporting Fig. 4A).

Because PI3K/pAkt are upstream of I kappa B kinase (IKK) and the IKK complex is central for the activation of nuclear factor kappa light-chain enhancer of activated B cells (NF $\kappa$ B) to regulate collagen I,<sup>26,31</sup> we focused on analyzing this signaling pathway. There was up-regulation of the ratios pIKK $\alpha,\beta$ ,<sup>176/180</sup>Ser/IKK $\alpha,\beta$ , and pI $\kappa$ B $\alpha$ <sup>32</sup>Ser/I $\kappa$ B $\alpha$ , as well as of nuclear/cytosolic p65, in OPN-treated rat HSC (Fig. 2C). However, involvement of the target of rapamycin/70-kDa ribosomal protein S6 kinase (mTOR-p70S6K) cascade, a translational regulatory mechanism downstream of PI3K and pAkt<sup>473</sup>Ser for regulating collagen I,<sup>32</sup> was precluded, because rOPN neither altered mTOR and p70S6K expression (Fig. 2D) nor induced mTOR phosphorylation at<sup>2448</sup>Ser or<sup>2481</sup>Ser in rat HSCs (undetectable).

To further define the molecular mechanism for collagen I induction under rOPN challenge, we evaluated the potential role of the activation of these two stress-sensitive kinases (i.e., PI3K and pAkt) and of the NF $\kappa$ B-signaling pathway. Wortmannin, a PI3K inhibitor, neither altered rat HSC viability (100% by the 3-(4,5-dimethylthiazol-2-yl)-2,5-diphenyltetrazolium bromide assay), morphology nor proliferation rates (Supporting Fig. 4B and not shown); however, three different doses of wortmannin down-regulated total collagen I expression in rat HSCs cotreated with rOPN (Fig. 3A, top). Similar effects were observed by coincubation with LY294002, a second PI3K inhibitor (Fig. 3A, bottom), thus linking OPN, PI3K-pAkt activation, and collagen I up-regulation in rat HSCs. Comparable results were observed in human HSCs (Supporting Fig. 4C). Last, inhibitors of pp38, pERK1/2, and pJNK signaling did not prevent the increase in collagen I by rOPN (not shown).

Addition of pyrrolidine dithiocarbamate (PDTC) to block NF $\kappa$ B signaling prevented the rOPN-driven increase in collagen I in rat HSC (Fig. 3B, top). Analogous effects were observed by coincubation with CAY10512—a second inhibitor of NF $\kappa$ B signaling (Fig. 3B, middle). Moreover, HSC infected with Ad-NF $\kappa$ B-Luc and treated with rOPN for 24 hours showed a 2-fold increase in luciferase activity, compared to non-rOPN-treated, Ad-NF $\kappa$ B-Luc-infected cells (Fig. 3B, bottom). Both wortmannin and an  $\alpha_v\beta_3$  integrin neutralizing Ab blunted the rOPN-mediated effect on the ratios, pIKK $\alpha,\beta$ ,<sup>176/180</sup>Ser/IKK $\alpha,\beta$ , and pI $\kappa$ B $\alpha$ <sup>32</sup>Ser/I $\kappa$ B $\alpha$ , as well as on nuclear/cytosolic p65 (Fig. 3C), suggesting engagement of OPN with integrin  $\alpha_v\beta_3$ , PI3K-pAkt activation, and NF $\kappa$ B signaling

F3

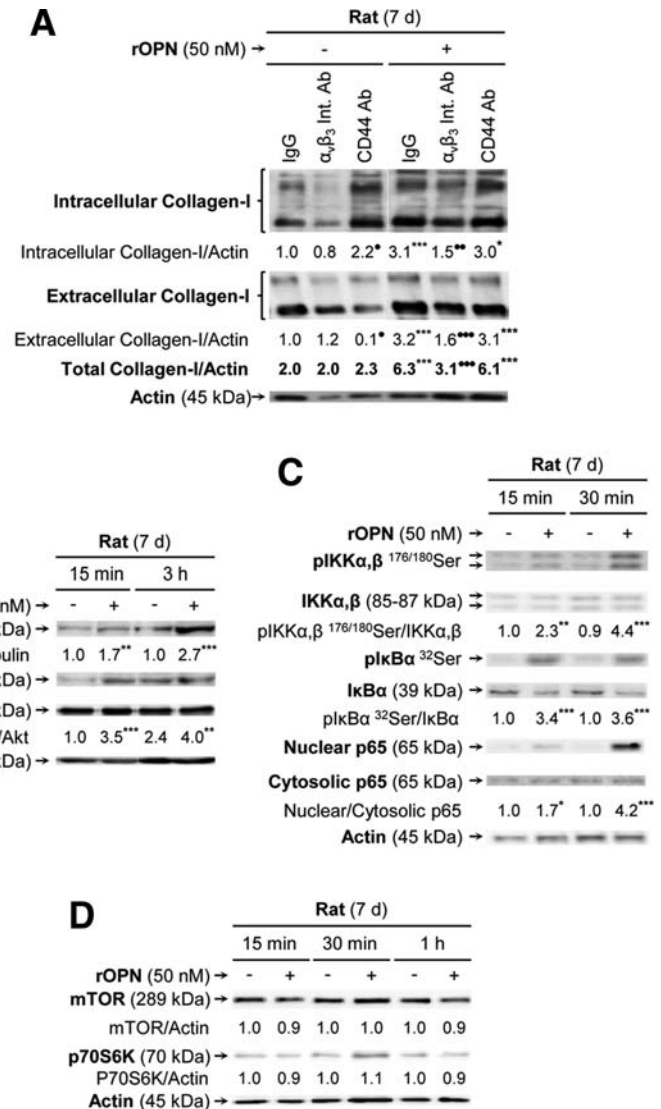


Fig. 2. Role of  $\alpha_v\beta_3$  integrin and the PI3K/pAkt/NF $\kappa$ B-signaling pathway in the rOPN-mediated effects on collagen I. Primary rat HSCs cultured for 7 days were incubated with 0-50 nM of rOPN plus 5  $\mu$ g/mL of non-mune immunoglobulin G (IgG), anti- $\alpha_v\beta_3$ , or anti-CD44 for 6 hours. Western blotting analysis of intra- and extracellular collagen I and actin (A). Western blotting analysis of PI3K, pAkt<sup>473</sup>Ser, Akt, and  $\beta$ -tubulin up to 3 hours of 0-50 nM of rOPN treatment in rat HSCs (B). Western blotting analysis of pIKK $\alpha,\beta$ <sup>176/180</sup>Ser, IKK $\alpha,\beta$ , pI $\kappa$ B $\alpha$ <sup>32</sup>Ser, I $\kappa$ B $\alpha$ , nuclear and cytosolic p65, and actin up to 30 minutes of 0-50 nM of rOPN treatment in rat HSCs (C). Western blotting analysis of mTOR, p70S6K, and actin up to 1 hour of 0-50 nM of rOPN treatment in rat HSCs (D). Results are expressed as average values. Experiments were performed in triplicate four times. \* $P$  < 0.05, \*\* $P$  < 0.01, and \*\*\* $P$  < 0.001 for rOPN-treated versus control at any given time point. ● $P$  < 0.05, ●● $P$  < 0.01 and ●●● $P$  < 0.001 for cotreated versus Ab treated.

to up-regulate collagen I expression in rat HSCs. Last, blocking  $\alpha_v\beta_3$  integrin prevented the increase in PI3K, the ratio, pAkt<sup>473</sup>Ser/Akt, and collagen I by rOPN in rat HSCs (Fig. 3D). In summary, these results established a connection among rOPN,  $\alpha_v\beta_3$  integrin, PI3K-pAkt activation, and the NF $\kappa$ B-signaling pathway to drive collagen I up-regulation in rat HSCs in a paracrine manner.

**OPN Expression Is Up-regulated in Liver Fibrosis.** Samples from stage 3 hepatitis C virus (HCV) cirrhotic patients displayed a correlation between elevated collagen I and cleaved OPN protein (~55-, ~42-, and ~25-kDa isoforms), compared to healthy individuals. Fully modified (glycosylated and phosphorylated) monomeric OPN, typically running at ~75 kDa, was not detectable (Fig. 4A).

To determine whether OPN also increased during liver injury in mice, we used well-established *in vivo*

models to induce liver fibrosis, such as CCl<sub>4</sub> injection and thioacetamide (TAA) treatment.<sup>33</sup> These drugs undergo cytochrome P450 metabolism leading to significant oxidant stress, inflammation, and hepatocyte necrosis within hours. The ~25-kDa OPN form was markedly induced in acute and chronic models of liver injury, whereas the ~55-kDa OPN form was elevated only under chronic CCl<sub>4</sub> injection and TAA treatment (Fig. 4B). Hence, there was an association between OPN induction, OPN proteolytic processing, and extent of liver fibrosis, both in humans and in mice.

Next, we evaluated the specific localization of the OPN induction in the liver. Nontreated livers showed OPN<sup>+</sup> biliary epithelial cells (not shown). Primary HSCs isolated from WT mice and cultured for 6 days were OPN<sup>+</sup> (Fig. 4C, left). Immunohistochemical (IHC) analysis revealed OPN expression in HSC,<sup>30</sup> biliary epithelial cells,<sup>4,6,34</sup> oval cells, and, mostly, in

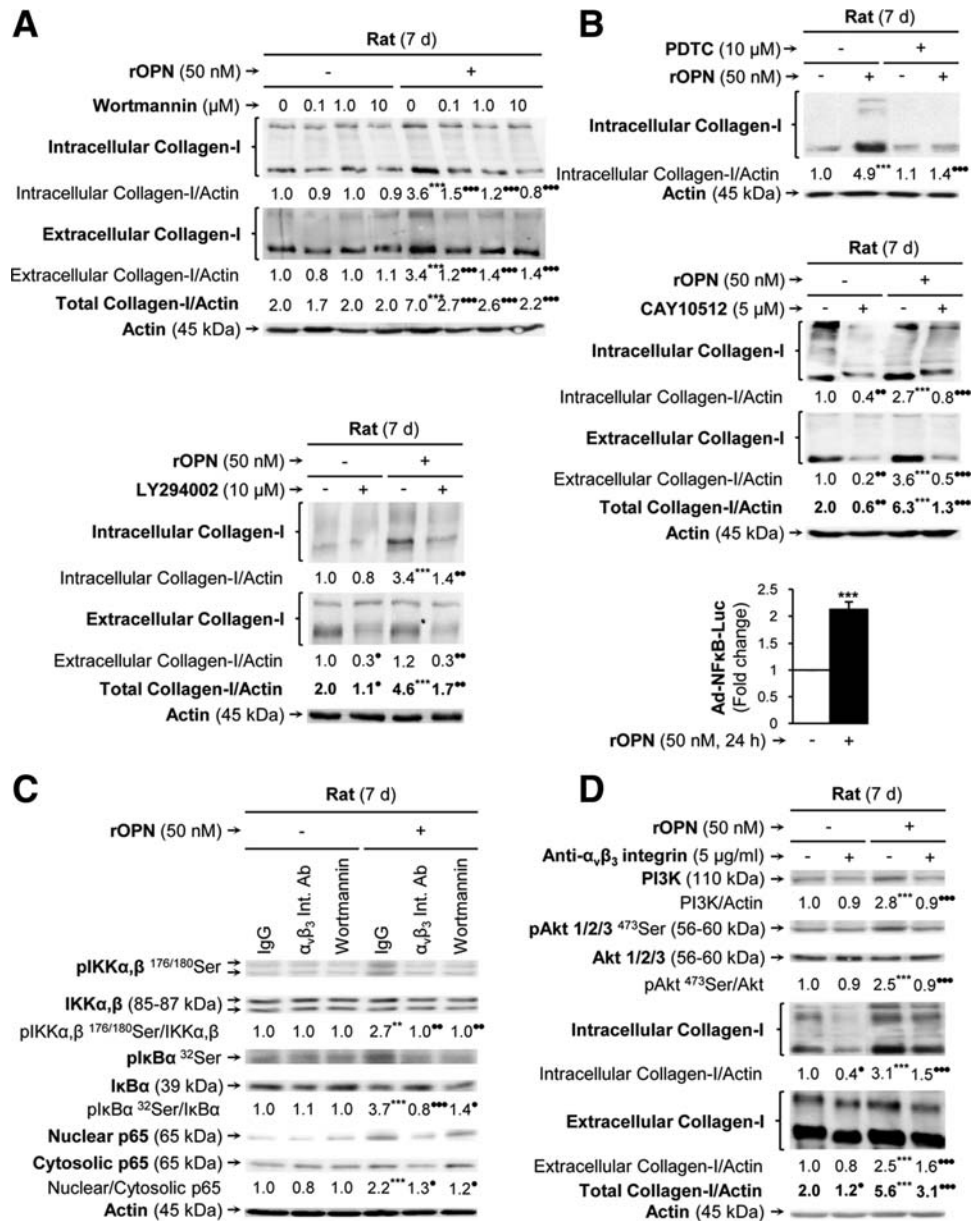


Fig. 3. Blocking  $\alpha_v\beta_3$  integrin, PI3K-pAkt activation, and the NF $\kappa$ B-signaling pathway prevents rOPN-mediated effects on collagen I. Primary rat HSCs cultured for 7 days were treated with 0-50 nM of rOPN or cotreated with 0-10  $\mu$ M of wortmannin, 0-10  $\mu$ M of LY294002, 0-10  $\mu$ M of PDTC, 0-5  $\mu$ M of CAY10512, or with 5  $\mu$ g/mL of nonimmune IgG or a neutralizing Ab to integrin  $\alpha_v\beta_3$ . Western blotting analysis showing that the rOPN-mediated induction of collagen I in HSCs was blunted by 0.1, 1, and 10  $\mu$ M of wortmannin (A, top), LY294002 (A, bottom), PDTC (B, top), and CAY10512 (B, middle). Infection of HSCs with Ad-NF $\kappa$ B-Luc for 48 hours and treatment with 50 nM of rOPN for 24 hours increased luciferase activity over that of nontreated Ad-NF $\kappa$ B-Luc-infected cells (B, bottom). Both integrin  $\alpha_v\beta_3$  Ab and wortmannin blunted the rOPN-mediated induction of the ratios, pIKK $\alpha,\beta$ <sup>176/180</sup>Ser/IKK $\alpha,\beta$ , pIkBa<sup>32</sup>Ser/IkBa, and nuclear/cytosolic p65 (C). Neutralizing Ab to integrin  $\alpha_v\beta_3$  prevented the induction of PI3K, the ratio pAkt<sup>473</sup>Ser/Akt, and collagen I by rOPN in HSCs (D). Results are expressed as average values. Experiments were performed in triplicate four times. \*\* $P$  < 0.01 and \*\*\* $P$  < 0.001 for rOPN-treated versus control. ● $P$  < 0.05, ●● $P$  < 0.01, and ●●● $P$  < 0.001 for inhibitor or Ab cotreated versus rOPN treated or control.

damaged hepatocytes in WT mice injected with CCl<sub>4</sub> for 1 month (Figure 4C, middle). Similar results were observed under TAA treatment, although hepatocytes showed punctated staining (Fig. 4C, right). Insets show OPN<sup>+</sup> HSCs in both models. In the early stages of CCl<sub>4</sub>- and TAA-mediated liver injury, Kupffer cells were also OPN<sup>+</sup> (not shown); however, the staining faded with disease progres-

sion. Of note, granular OPN<sup>+</sup> staining—typical of secreted proteins—appeared in focal-septal hepatocytes (Fig. 4C, middle). There was colocalization of OPN<sup>+</sup> staining with  $\alpha$ -SMA<sup>+</sup> (an HSC activation marker) under TAA treatment (Fig. 4D) and by CCl<sub>4</sub> injection (not shown).

Because liver fibrosis is associated with significant oxidant stress, to dissect whether OPN was responsive

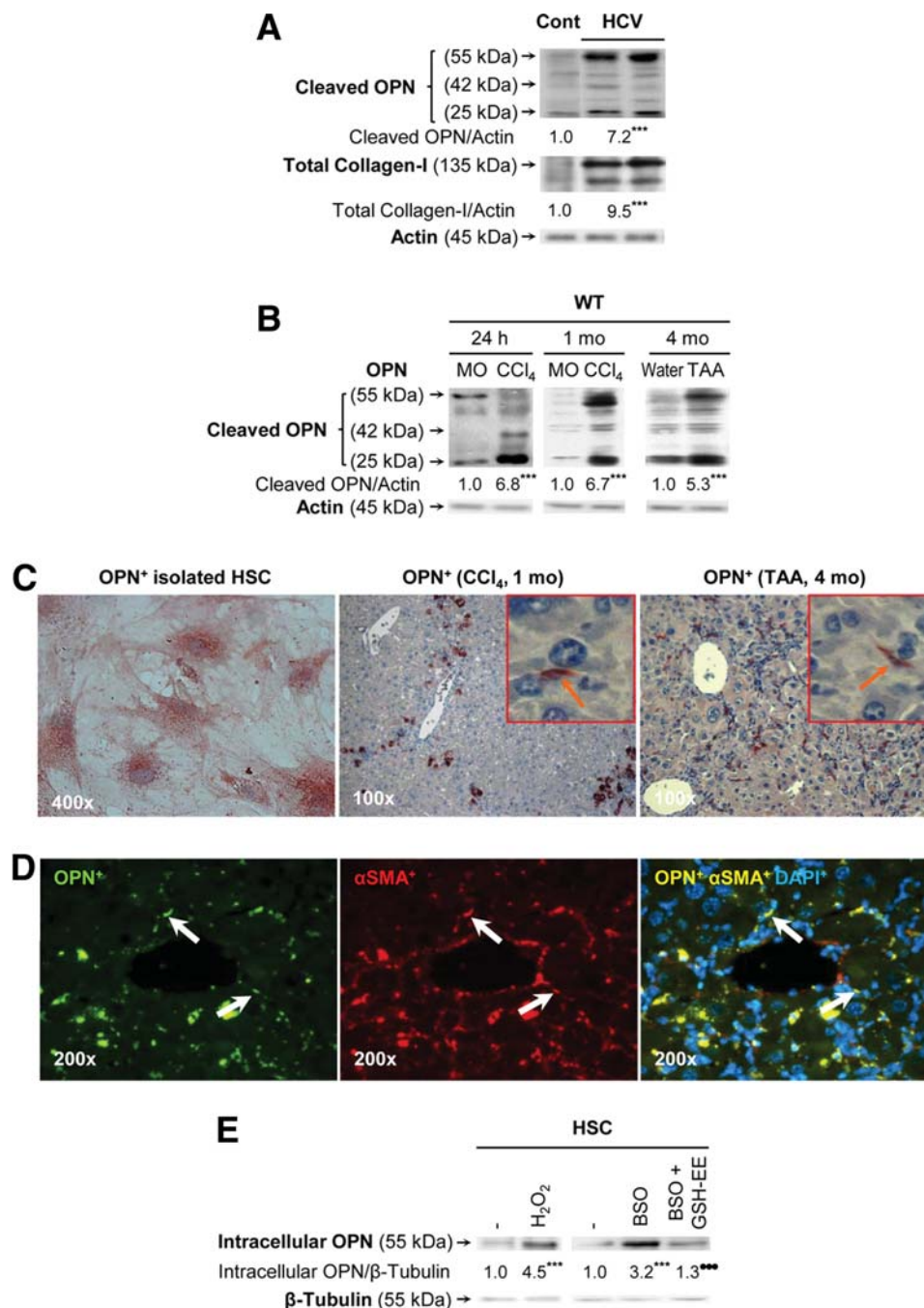


Fig. 4. OPN expression is induced during liver injury and under oxidant stress conditions. Western blotting analysis of cleaved OPN, total collagen I, and actin in livers from control and from patients with stage 3 HCV-induced cirrhosis (A). Western blotting analysis of cleaved OPN and actin in livers of mice injected with CCl<sub>4</sub> for 24 hours (acute liver injury), with CCl<sub>4</sub> for 1 month, or with TAA for 4 months (chronic liver injury) (B). In (A) and (B), fully modified (glycosylated and phosphorylated) monomeric OPN was not detected. IHC for OPN in primary HSCs isolated from WT mice and cultured for 6 days (C, left). IHC depicting significant OPN expression in HSCs, biliary epithelial cells, and hepatocytes at 1 month of CCl<sub>4</sub> injection (C, middle) and in HSCs, biliary epithelial cells, oval cells, and hepatocytes after 4 months of TAA treatment (C, right). Insets show OPN<sup>+</sup> HSCs in both models (→). Immunofluorescence showing colocalization of OPN<sup>+</sup> with α-SMA<sup>+</sup> (an HSC activation marker) after 4 months of TAA treatment (D). Western blotting analysis of intracellular OPN and β-tubulin in HSCs in the presence of two prooxidants (H<sub>2</sub>O<sub>2</sub> and BSO) and an antioxidant (GSH-EE) (E). Results are expressed as average values. Experiments were performed in triplicate four times. \*\*\*P < 0.001 for HCV, CCl<sub>4</sub>, TAA, or prooxidant treated versus control, mineral oil (MO), or water, respectively. ●●●P < 0.001 for BSO+GSH-EE cotreated versus BSO treated.

to reactive oxygen species, HSC were challenged with H<sub>2</sub>O<sub>2</sub>—a prooxidant typically generated during CCl<sub>4</sub> metabolism—or with L-buthionine sulfoximine (BSO), which depletes glutathione (GSH). Both treat-

ments increased OPN expression in HSC, whereas cotreatment with GSH-EE (ethyl ester) to restore GSH levels, blunted this effect (Fig. 4E). To validate the induction of OPN by oxidant stress *in vivo*, WT

C  
O  
L  
O  
R

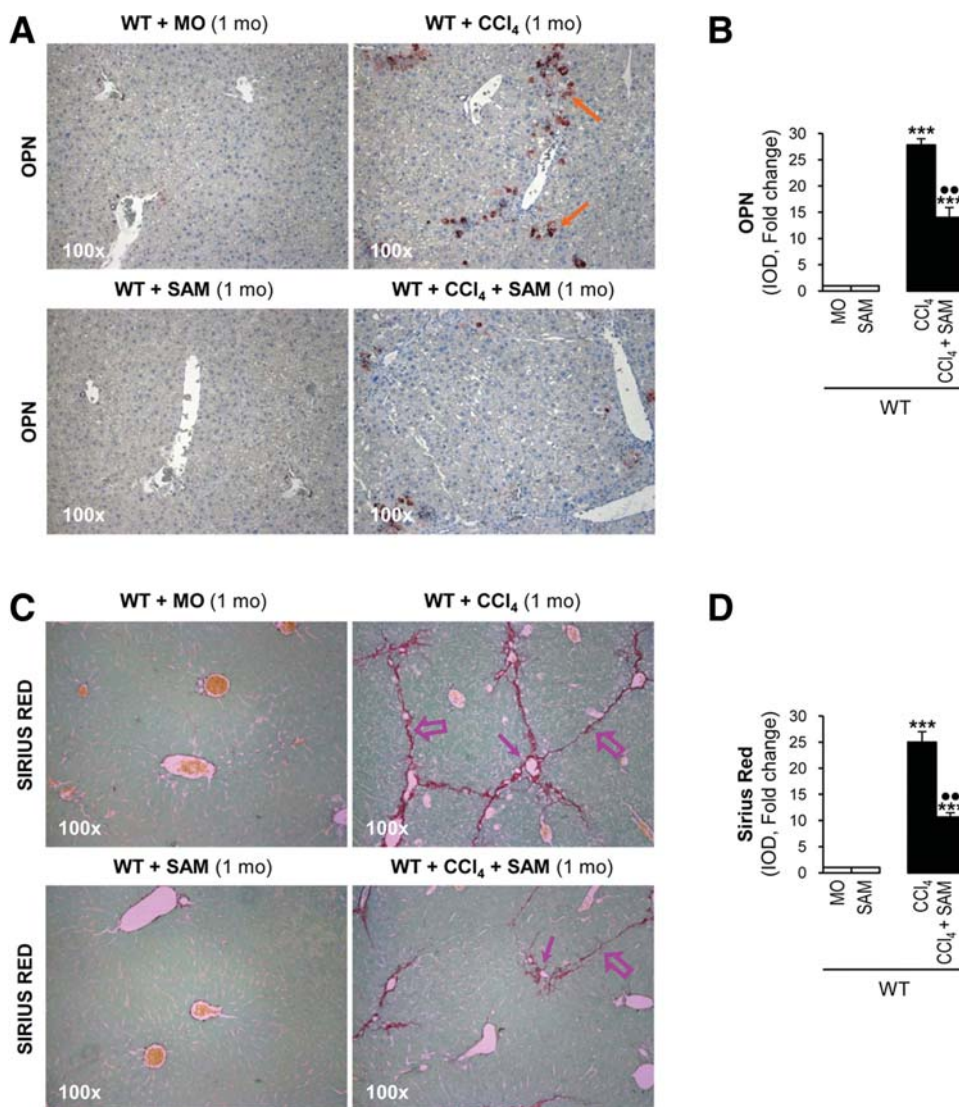


Fig. 5. SAM protects WT mice from CCl<sub>4</sub>-induced chronic liver injury. C57BL/6J WT mice were injected MO, SAM+MO, CCl<sub>4</sub>, or CCl<sub>4</sub>+SAM for 1 month. Cotreated mice showed decreased OPN expression (A), which was quantified by morphometry analysis (B). Likewise, fibrosis was less apparent in cotreated mice than in CCl<sub>4</sub>-injected mice, as shown by Sirius red/fast green staining (C) and morphometry analysis (D). Results are expressed as mean values ± standard error of the mean (SEM). n = 8/group; \*\*\*P < 0.001 for CCl<sub>4</sub> or CCl<sub>4</sub>+SAM versus MO or SAM; ●●P < 0.01 for CCl<sub>4</sub>+SAM versus CCl<sub>4</sub>.

COLOR

mice were CCl<sub>4</sub> injected for 1 month in the presence or absence of S-adenosylmethionine (SAM), an antioxidant known to restore GSH levels. Coinjection with SAM lowered OPN protein (Fig. 5A,B) and the extent of liver fibrosis (Fig. 5C,D) by 50%, when compared to mice injected with CCl<sub>4</sub> alone. In summary, these data proved the ability of OPN to respond to drug-induced liver injury and to oxidant stress.

**WT Show More CCl<sub>4</sub>-Induced Chronic Liver Injury and Fibrosis Than *Opn*<sup>-/-</sup> Mice.** Fibrosis typically develops as a result of chronic liver injury. To decipher the role of OPN in the progression of liver disease, we tested whether chronic CCl<sub>4</sub> injection could lead to differences in the extent of liver fibrosis. CCl<sub>4</sub>-injected C57BL/6J WT showed greater alanine aminotransferase (ALT) activity and more inflammation, hepatocyte-ballooning degeneration, and necrosis than *Opn*<sup>-/-</sup> mice (Fig. 6A-E). Cytochrome P450 2E1 (CYP2E1) expression was similar in WT and *Opn*<sup>-/-</sup> mice, indicating that

the extent of liver injury in these mice was not the result of different CCl<sub>4</sub> metabolism (Fig. 6F).

In addition, CCl<sub>4</sub>-injected WT mice presented elevated collagenous proteins, portal fibrosis, bridging fibrosis, scar thickness, Brunt fibrosis score, and Sirius red and collagen I morphometry, compared to *Opn*<sup>-/-</sup> mice (Fig. 7A-E). The above-described results were validated in WT and *Opn*<sup>-/-</sup> 129sv mice (Supporting Figs. 5 and 6). Transgenic mice overexpressing OPN in hepatocytes (*Opn*<sup>HEP</sup> Tg) and injected with CCl<sub>4</sub> for 1 month showed similar ALT activity, necrosis, and inflammation, but significant periportal, bridging, and sinusoidal fibrosis, along with increased collagen I scar thickness, compared to WT mice (Fig. 8). Moreover, *Opn*<sup>HEP</sup> Tg mice developed spontaneous perivenular, perisinusoidal, and portal fibrosis over time (1 year) in the absence of any profibrogenic treatment (Supporting Fig. 7). In aggregate, the data suggest that OPN plays a major role in chronic CCl<sub>4</sub>-induced hepatic fibrosis by regulating scar formation.

F7

F8

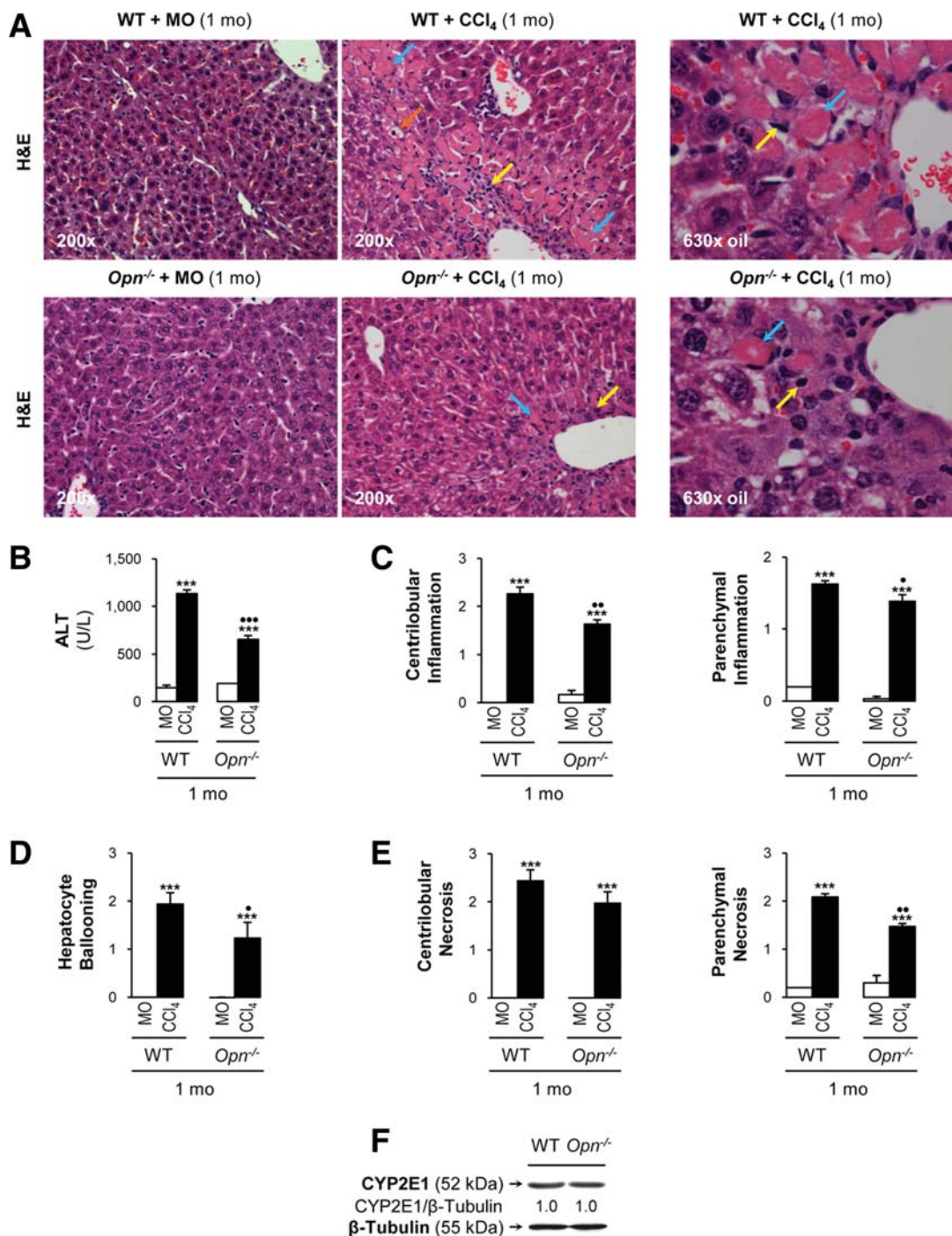
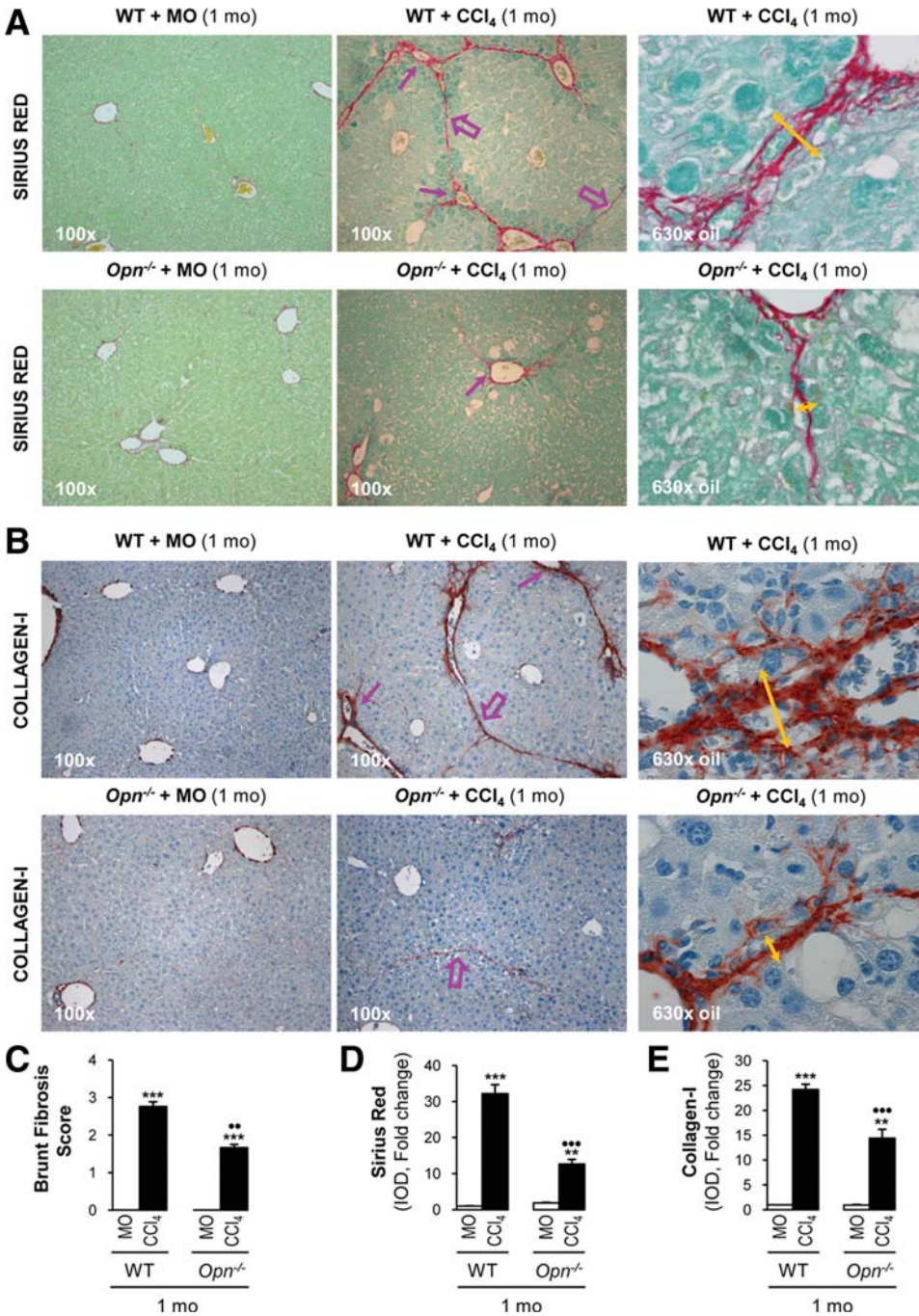


Fig. 6. WT mice show more CCl<sub>4</sub>-induced chronic liver injury than Opn<sup>-/-</sup> mice. C57BL/6J WT and Opn<sup>-/-</sup> mice were injected with CCl<sub>4</sub> or MO for 1 month. Hematoxylin and eosin (H&E) staining revealed more centrilobular necrosis (➔), centrilobular inflammation (➡), and hepatocyte-ballooning degeneration (➞) in CCl<sub>4</sub>-injected WT than in Opn<sup>-/-</sup> mice (A). ALT activity (B), centrilobular, and parenchymal inflammation scores (C), hepatocyte-ballooning degeneration score (D), and centrilobular and parenchymal necrosis scores (E). Western blotting analysis showing similar CYP2E1 expression in WT and Opn<sup>-/-</sup> mice (F). Results are expressed as mean values ± SEM. n = 8/group; \*\*\*P < 0.001 for CCl<sub>4</sub> versus MO; ●P < 0.05, ●●P < 0.01, and ●●●P < 0.001 for Opn<sup>-/-</sup>+CCl<sub>4</sub> versus WT+CCl<sub>4</sub>.

**WT Mice Show Significant Liver Fibrosis Under Chronic TAA Treatment, Compared to Opn<sup>-/-</sup> Mice.** To confirm the results obtained under chronic CCl<sub>4</sub> injection, we used TAA treatment as a second model of chronic drug-induced liver fibrosis. Sirius

red/fast green staining and collagen I IHC showed stage >3 fibrosis in TAA-treated WT and ~1-2 in Opn<sup>-/-</sup> mice with clear induction of collagen I deposition in TAA-treated WT, compared to Opn<sup>-/-</sup> mice, extensive portal fibrosis, bridging fibrosis, and a

C  
O  
L  
O  
R



COLOR

Fig. 7. WT mice show more CCl<sub>4</sub>-induced liver fibrosis than Opn<sup>-/-</sup> mice. C57BL/6J WT and Opn<sup>-/-</sup> mice were injected CCl<sub>4</sub> or MO for 1 month. Sirius red/fast green staining indicated fibrosis stage ~3 in CCl<sub>4</sub>-injected WT and ~1-2 in CCl<sub>4</sub>-injected Opn<sup>-/-</sup> mice (portal  $\blacktriangleright$  and bridging  $\Rightarrow$  fibrosis) as well as greater scar thickness in WT, compared to Opn<sup>-/-</sup> mice ( $\leftrightarrow$ ) (A). Collagen I IHC confirmed the extent of portal fibrosis ( $\blacktriangleright$ ), bridging fibrosis ( $\Rightarrow$ ), and scar thickness ( $\leftrightarrow$ ) in CCl<sub>4</sub>-injected mice (B). Brunt fibrosis score (C), Sirius red morphometry (D), and collagen I morphometry analysis (E). Results are expressed as mean values  $\pm$  SEM.  $n = 8$ /group; \*\* $P < 0.01$  and \*\*\* $P < 0.001$  for CCl<sub>4</sub> versus MO; ●● $P < 0.01$  and ●●● $P < 0.001$  for Opn<sup>-/-</sup>+CCl<sub>4</sub> versus WT+CCl<sub>4</sub>.

~3-fold increase in scar thickness (Supporting Fig. 8A,B). Thus, fibrosis was more distinct in TAA-treated WT, than in Opn<sup>-/-</sup> mice, as quantified by Brunt fibrosis score and by Sirius red and collagen I morphometry (Supporting Fig. 8C-E).

Collectively, these results suggest that increased OPN expression *per se* or after chronic liver injury and oxidant stress can stimulate collagen I deposition *in vivo*. In addition, the *in vitro* studies demonstrate that intracellular OPN plays an autocrine role in regulating collagen I expression in HSCs. Moreover, treatment

with rOPN to resemble the paracrine actions of secreted OPN increases HSC invasion, chemotaxis, and wound-healing potential and up-regulates collagen I via integrin  $\alpha_v\beta_3$  engagement, activation of PI3K-pAkt, and NF $\kappa$ B signaling (Supporting Fig. 9).

## Discussion

It is becoming clearer that OPN is significantly induced during liver injury, both in humans and in rodents.<sup>4-6,17</sup> In the past few years, work from several

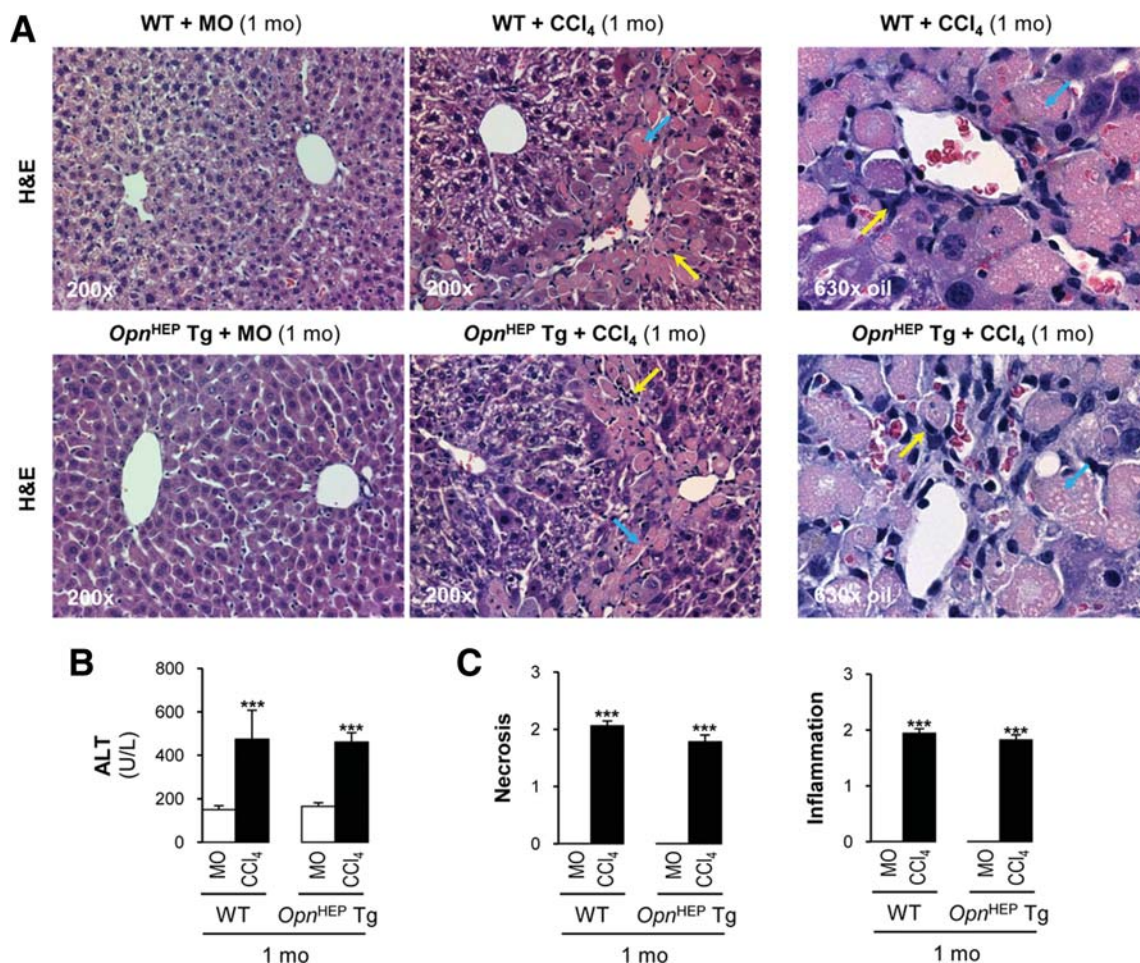


Fig. 8. *Opn*<sup>HEP Tg</sup> mice in C57BL/6J genetic background show more CCl<sub>4</sub>-induced fibrosis than WT mice. WT and *Opn*<sup>HEP Tg</sup> mice were injected with MO or CCl<sub>4</sub> for 1 month. H&E staining revealed similar centrilobular necrosis (↔) and inflammation (↘) in CCl<sub>4</sub>-injected *Opn*<sup>HEP Tg</sup> and in WT mice (A). ALT activity (B). Necrosis and inflammation scores (C). Sirius red/fast green staining and IHC for collagen I demonstrated more portal fibrosis (↗), bridging fibrosis (↔), and sinusoidal fibrosis (↘) in CCl<sub>4</sub>-injected *Opn*<sup>HEP Tg</sup> than in WT mice (D and E). Brunt fibrosis score, collagen I, and Sirius red/fast green morphometry (F). Results are expressed as mean values ± SEM. *n* = 8/group; \*\**P* < 0.01 and \*\*\**P* < 0.001 for CCl<sub>4</sub> versus MO; ●●*P* < 0.01 for *Opn*<sup>HEP Tg</sup>+CCl<sub>4</sub> versus WT+CCl<sub>4</sub>.

C  
O  
L  
O  
R

groups<sup>4-6,17</sup> studied the potential role of OPN in liver fibrosis, albeit with inconclusive results. Studies by Lee et al.<sup>5</sup> demonstrated an OPN increase in culture medium from culture-activated HSCs and under oral CCl<sub>4</sub> administration; however, no mechanistic studies were performed to dissect how OPN regulates collagen I protein deposition. Lorena et al.<sup>6</sup> suggested increased susceptibility to CCl<sub>4</sub> injection in *Opn*<sup>-/-</sup> mice. Although the investigators claimed that the protection observed in WT mice was the result of enhancement of hepatocyte survival and reduction in type 2 nitric oxide synthase (NOS2) expression; yet, they neither provided IHC for cell-survival markers nor measured the concentration of NO· or ONOO<sup>-</sup> to support their conclusions, and no studies on collagen I regulation were performed. Last, a recent publication from Syn et al.<sup>4</sup> proposes a role for the Hedgehog-signaling pathway in activating OPN and promoting fibrosis

progression in nonalcoholic steatohepatitis; however, it is not clear which OPN isoform the investigators were referring to, and it is *Gli1*, and not *Gli2*, expression that it is widely considered the most reliable readout for cells undergoing active Hedgehog signaling.

Thus, there is a well-timed need for dissecting the molecular mechanism on how this matricellular protein could regulate the fibrogenic response to liver injury and, specifically, collagen I protein expression by HSCs. Currently, there are many unresolved questions on how OPN could act as a feed-forward mechanism to promote scarring, and among these are the following: Does extracellular OPN have the ability to increase HSC profibrogenic potential and HSC-derived collagen I protein?; which HSC receptors are involved in the profibrogenic cascade triggered by OPN?; what intracellular signals are activated upon OPN-receptor binding that drive the collagen I

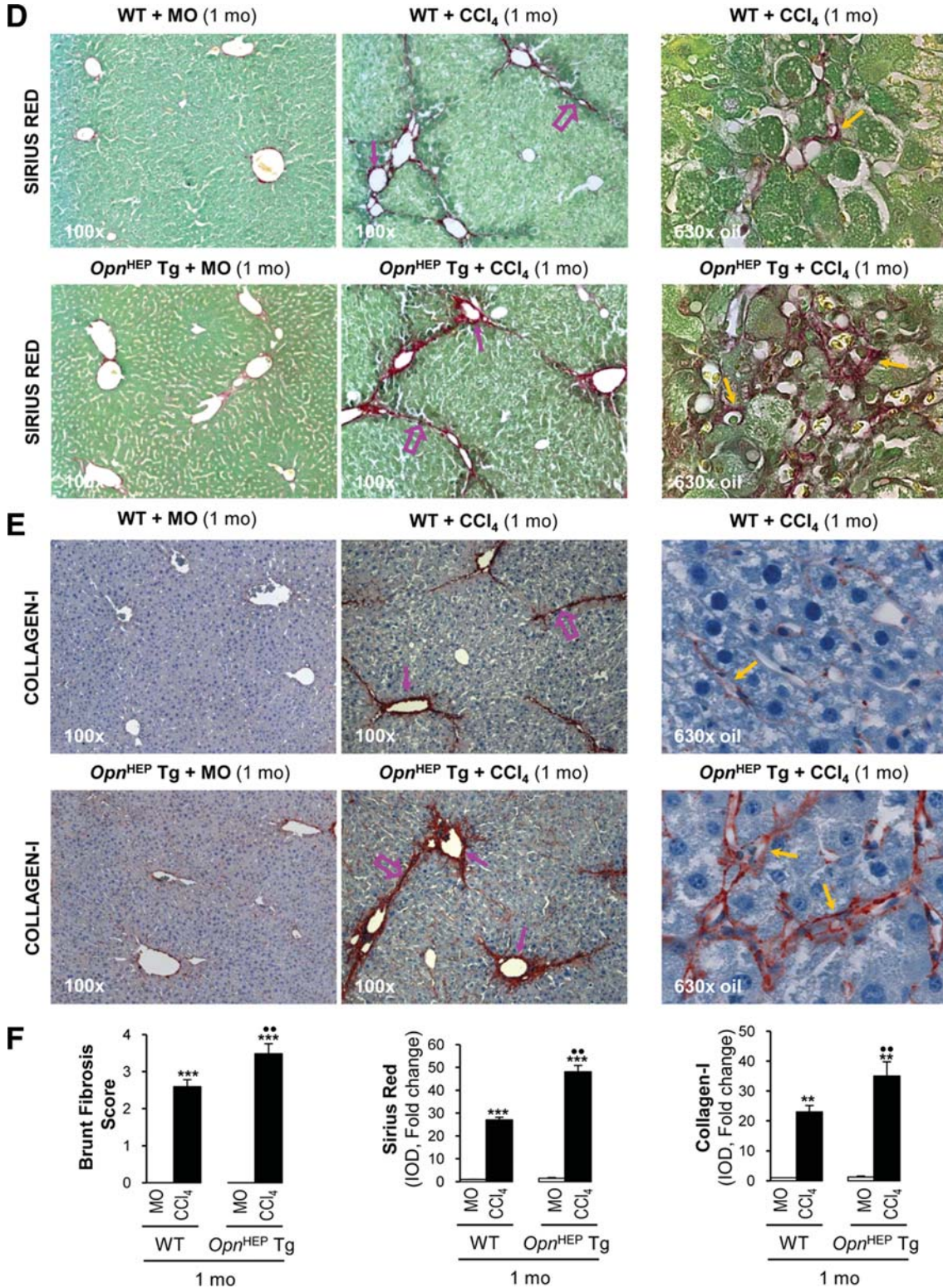


Fig. 8. (Continued).

increase in HSCs?; is autocrine OPN signaling involved in regulating collagen I in HSCs?; is OPN sensitive to oxidant stress?; which OPN isoforms appear during the course of liver fibrosis?; and does OPN induce sinusoidal fibrosis?.

Thus, the overall aim of this work was to address these questions, identify the mechanism for the OPN-driven collagen I up-regulation in HSCs, and determine the functional role of OPN in the pathogenesis of liver fibrosis. The idea that OPN mediates liver

COLOR

fibrosis is relevant for several reasons. First, because the observation that OPN is up-regulated in HSCs during hepatic injury provides an excellent conceptual advance in our understanding of liver fibrogenesis, as it appears that OPN up-regulates HSC collagen I protein in an autocrine and paracrine fashion. Second, it supports the clinicopathological finding that injury occurring in the central region is accompanied by fibrosis. Third, it opens the possibility of linking a soluble cytokine/matrix protein with fibrogenesis. Last, the identification of the mechanism and mediators involved in the profibrogenic actions of OPN could help in devising strategies for therapeutic targeting.

Our *in vitro* experiments validated the hypothesis of the profibrogenic and proinvasive actions of OPN in HSC. Mechanistic studies identified the HSC membrane proteins engaged by OPN and the proximal signaling molecules/oxidant stress-sensitive kinases activated upon OPN binding that trigger the fibrogenic cascade. The experimental data identified integrin  $\alpha_v\beta_3$  as an efficient conveyor of the OPN-mediated profibrogenic actions in HSC and pointed at PI3K-pAkt activation and the NF $\kappa$ B-signaling pathway as highly involved in this process.

Because OPN signals via integrins and CD44, it is feasible that after liver injury, a ligand for  $\alpha_v\beta_3$  integrin, such as OPN, accumulates in the space of Disse and acts in a  $\alpha_v\beta_3$  integrin-dependent manner to maintain collagen I induction, HSC activation, invasion, and migration. Because OPN binds ECM proteins,<sup>35,36</sup> this binding ability may enhance HSC activation, migration, and invasion—key HSC features for the development of fibrosis. The finding that blocking CD44 did not prevent the effect of rOPN on collagen I may be related to the ability of hyaluronic acid—a glycosaminoglycan synthesized during HSC activation<sup>24,37</sup>—to bind CD44; thus, competitive inhibition between hyaluronic acid and rOPN for CD44 binding could occur in HSCs, although this possibility needs further investigation.

Several observations support the role for PI3K-pAkt activation and the NF $\kappa$ B-signaling pathway in the effects mediated by rOPN on collagen I. First, rOPN rapidly increased PI3K, the ratios pAkt<sup>473</sup>Ser/Akt, pIKK $\alpha,\beta$ <sup>176/180</sup>Ser/IKK $\alpha,\beta$ , and pI $\kappa$ B $\alpha$ <sup>32</sup>Ser/I $\kappa$ B $\alpha$ , as well as nuclear translocation of p65. Second, inhibitors of PI3K activation and NF $\kappa$ B signaling blunted the rOPN-mediated increase in intra- and extracellular collagen I protein. Third, blockade of  $\alpha_v\beta_3$  integrin signaling with a neutralizing Ab and incubation with wortmannin or LY294002 prevented the induction of PI3K, the increase in the ratios, pAkt<sup>473</sup>Ser/Akt,

pIKK $\alpha,\beta$ <sup>176/180</sup>Ser/IKK $\alpha,\beta$ , and pI $\kappa$ B $\alpha$ <sup>32</sup>Ser/I $\kappa$ B $\alpha$ , nuclear translocation of p65, and the up-regulation of collagen I protein by rOPN. Involvement of the mTOR cascade was ruled out, because rOPN altered neither mTOR-p70S6K expression nor mTOR phosphorylation. Therefore, this study linked extracellular and/or secreted OPN (i.e., paracrine effect) with  $\alpha_v\beta_3$  integrin binding, PI3K-pAkt activation, NF $\kappa$ B signaling, and scarring.

Work from several laboratories,<sup>3-6</sup> including our own, suggests that HSCs are an important source of OPN during liver injury. To date, OPN was believed to exert its effects by binding the RGD motif in integrins and the cell-surface receptor, CD44; however, an intracellular function of OPN in liver fibrosis was largely unknown. Because HSCs isolated from *Opn*<sup>-/-</sup> mice were less profibrogenic than those from WT mice and infection of HSC with Ad-OPN increased intracellular collagen I, these results suggested a novel autocrine mechanism whereby intracellular OPN could modulate collagen I deposition in HSCs. Alternatively, extracellular OPN, either from HSCs or from neighboring cells, may activate HSCs through its receptor ( $\alpha_v\beta_3$  integrin), as suggested above, thus creating a positive feedback loop.

To further validate our hypothesis, we then assessed whether OPN contributed to the fibrogenic response *in vivo* using two mouse models of drug-induced liver injury. The data from human samples and from the mouse models showed that most of the OPN found in liver injury appeared to have been cleaved at least at the endpoint of the experiments. The role of each cleaved isoform in regulating the fibrogenic response to liver injury, as well as the identification of the proteases that cleave hepatic OPN, is currently under active investigation in our laboratory, because additional integrin-binding sites, other than  $\alpha_v\beta_3$  integrin, are likely to be uncovered by proteolytic processing of the protein.

Upon the onset of liver injury in mice, the increase in OPN likely results from oxidant stress because CCl<sub>4</sub> and TAA metabolism via CYPs generate a considerable amount of free radicals,<sup>33</sup> and the *in vitro* data demonstrated the OPN responsiveness to oxidant stress, which was blocked by antioxidant treatment. Furthermore, cotreatment with SAM, known to elevate GSH levels, prevented the increase in OPN and the fibrogenic response in WT mice injected with CCl<sub>4</sub> for 1 month.

Although it is possible that the chronic effects of *Opn* ablation could be secondary to its effects on liver injury itself (i.e., inflammation and ductular reaction, unpublished observations), the data clearly reveal a direct action of OPN on collagen I protein expression,

a key event in liver fibrosis. Hence, OPN appears to induce scarring *per se*. This is, indeed, also supported by the finding that though ALT activity and the necrosis and inflammation scores were similar, there was increased portal, bridging, and sinusoidal fibrosis, along with enhanced width of the collagenous septa in CCl<sub>4</sub>-injected *Opn*<sup>HEP</sup> Tg mice, compared to their WT littermates. Notably, *Opn*<sup>HEP</sup> Tg mice developed spontaneous fibrosis over time, whereas WT mice did not. Last, in line with the results using *Opn*<sup>HEP</sup> Tg mice and the *in vitro* data, fibrillar collagen I content and scar thickness was significantly lowered by OPN ablation *in vivo*. It is likely that secreted OPN allows paracrine signaling to HSC, whereas endogenous OPN expression in HSCs signals in an autocrine fashion, amplifying fibrogenic response. The cell- and matrix-binding ability of OPN may also facilitate a proper stromal and fibrillar collagen network organization. Overall, it is reasonable to propose that OPN may drive fibrogenic response, among others, by directly regulating collagen I deposition. Thus, OPN emerges as a key soluble cytokine and ECM-bound molecule promoting liver fibrosis.

**Acknowledgments:** The authors are very grateful to the following investigators: David T. Denhardt (Rutgers University, Newark, NJ) for his generous gift of the 2A1 Ab and for the *Opn*<sup>-/-</sup> mice in 129sv background; Satoshi Mochida (Saitama Medical University, Saitama, Japan) for providing the *Opn*<sup>HEP</sup> Tg mice; Andrea D. Branch (Mount Sinai School of Medicine, New York, NY) for donating the human liver protein lysates; Toshimitsu Uede (Hokkaido University, Sapporo, Japan) for the Ad-OPN and Ad-LacZ; John Engelhardt (University of Iowa, Iowa City, IA) for the recombinant Ad expressing the NFκB-Luc reporter; and Feng Hong (Mount Sinai School of Medicine) for supplying the primary human HSC isolated from normal liver margin of patients undergoing hepatic tumor resection.

The authors are also very thankful to all former and current members from the Nieto Laboratory for their helpful comments and suggestions throughout this project as well as for their critical review of the manuscript for this article. Special thanks go to Marcos Rojkind, Arthur I. Cederbaum, and David T. Denhardt for their constant support and for their very helpful insight throughout the course of this project.

## References

- Gäbele E, Brenner DA, Rippe RA. Liver fibrosis: signals leading to the amplification of the fibrogenic hepatic stellate cell. *Front Biosci* 2003;8:d69-d77.
- Milani S, Herbst H, Schuppan D, Kim KY, Riecken EO, Stein H. Procollagen expression by nonparenchymal rat liver cells in experimental biliary fibrosis. *Gastroenterology* 1990;98:175-184.
- De Minicis S, Seki E, Uchinami H, Kluwe J, Zhang Y, Brenner DA, Schwabe RF. Gene expression profiles during hepatic stellate cell activation in culture and *in vivo*. *Gastroenterology* 2007;132:1937-1946.
- Syn WK, Choi SS, Liaskou E, Karaca GF, Agboola KM, Oo YH, et al. Osteopontin is induced by hedgehog pathway activation and promotes fibrosis progression in nonalcoholic steatohepatitis. *HEPATOLOGY* 2011; 53:106-115.
- Lee SH, Seo GS, Park YN, Yoo TM, Sohn DH. Effects and regulation of osteopontin in rat hepatic stellate cells. *Biochem Pharmacol* 2004; 68:2367-2378.
- Lorena D, Darby IA, Gadeau AP, Leen LL, Rittling S, Porto LC, et al. Osteopontin expression in normal and fibrotic liver: altered liver healing in osteopontin-deficient mice. *J Hepatol* 2006;44:383-390.
- Kazanecki CC, Uzwiak DJ, Denhardt DT. Control of osteopontin signaling and function by post-translational phosphorylation and protein folding. *J Cell Biochem* 2007;102:912-924.
- Uede T. Osteopontin, intrinsic tissue regulator of intractable inflammatory diseases. *Pathol Int* 2011;61:265-280.
- Kazanecki CC, Kowalski AJ, Ding T, Rittling SR, Denhardt DT. Characterization of anti-osteopontin monoclonal antibodies: binding sensitivity to post-translational modifications. *J Cell Biochem* 2007;102: 925-935.
- El-Tanani MK, Campbell FC, Kurisetty V, Jin D, McCann M, Rudland PS. The regulation and role of osteopontin in malignant transformation and cancer. *Cytokine Growth Factor Rev* 2006;17:463-474.
- Apte UM, Banerjee A, McRee R, Wellberg E, Ramaiah SK. Role of osteopontin in hepatic neutrophil infiltration during alcoholic steatohepatitis. *Toxicol Appl Pharmacol* 2005;207:25-38.
- Banerjee A, Apte UM, Smith R, Ramaiah SK. Higher neutrophil infiltration mediated by osteopontin is a likely contributing factor to the increased susceptibility of females to alcoholic liver disease. *J Pathol* 2006;208:473-485.
- Ramaiah SK, Rittling S. Pathophysiological role of osteopontin in hepatic inflammation, toxicity, and cancer. *Toxicol Sci* 2008;103:4-13.
- Denhardt DT, Mistretta D, Chambers AF, Krishna S, Porter JF, Raghuram S, Rittling SR. Transcriptional regulation of osteopontin and the metastatic phenotype: evidence for a Ras-activated enhancer in the human OPN promoter. *Clin Exp Metastasis* 2003;20:77-84.
- Denhardt DT, Noda M, O'Regan AW, Pavlin D, Berman JS. Osteopontin as a means to cope with environmental insults: regulation of inflammation, tissue remodeling, and cell survival. *J Clin Invest* 2001; 107:1055-1061.
- Liaw L, Birk DE, Ballas CB, Whitsitt JS, Davidson JM, Hogan BL. Altered wound healing in mice lacking a functional osteopontin gene (spp1). *J Clin Invest* 1998;101:1468-1478.
- Fickert P, Stoger U, Fuchsbichler A, Moustafa T, Marschall HU, Weiglein AH, et al. A new xenobiotic-induced mouse model of sclerosing cholangitis and biliary fibrosis. *Am J Pathol* 2007;171:525-536.
- Schaefer B, Rivas-Estilla AM, Meraz-Cruz N, Reyes-Romero MA, Hernandez-Nazara ZH, Dominguez-Rosales JA, et al. Reciprocal modulation of matrix metalloproteinase-13 and type I collagen genes in rat hepatic stellate cells. *Am J Pathol* 2003;162:1771-1780.
- Cubero FJ, Nieto N. Ethanol and arachidonic acid synergize to activate Kupffer cells and modulate the fibrogenic response via tumor necrosis factor alpha, reduced glutathione, and transforming growth factor beta-dependent mechanisms. *HEPATOLOGY* 2008;48:2027-2039.
- Garcia-Trevijano ER, Iraburu MJ, Fontana L, Dominguez-Rosales JA, Auster A, Covarrubias-Pinedo A, Rojkind M. Transforming growth factor beta1 induces the expression of alpha1(I) procollagen mRNA by a hydrogen peroxide-C/EBPbeta-dependent mechanism in rat hepatic stellate cells. *HEPATOLOGY* 1999;29:960-970.
- Huang G, Brigstock DR. Integrin expression and function in the response of primary culture hepatic stellate cells to connective tissue growth factor (CCN2). *J Cell Mol Med* 2010;15:1087-1095.

22. Patsenker E, Popov Y, Stickel F, Schneider V, Ledermann M, Sagesser H, et al. Pharmacological inhibition of integrin alphavbeta3 aggravates experimental liver fibrosis and suppresses hepatic angiogenesis. *HEPATOLOGY* 2009;50:1501-1511.
23. Zhou X, Murphy FR, Gehdu N, Zhang J, Iredale JP, Benyon RC. Engagement of alphavbeta3 integrin regulates proliferation and apoptosis of hepatic stellate cells. *J Biol Chem* 2004;279:23996-24006.
24. Kikuchi S, Griffin CT, Wang SS, Bissell DM. Role of CD44 in epithelial wound repair: migration of rat hepatic stellate cells utilizes hyaluronic acid and CD44v6. *J Biol Chem* 2005;280:15398-15404.
25. Deng ZY, Li J, Jin Y, Chen XL, Lu XW. Effect of oxymatrine on the p38 mitogen-activated protein kinases signalling pathway in rats with CCl4 induced hepatic fibrosis. *Chin Med J (Engl)* 2009;122:1449-1454.
26. Nieto N. Ethanol and fish oil induce NFkappaB transactivation of the collagen alpha2(I) promoter through lipid peroxidation-driven activation of the PKC-PI3K-Akt pathway. *HEPATOLOGY* 2007;45:1433-1445.
27. Yuantai W, Tiancai W, Qiu Z. PD98059 inhibits expression of pERK1 protein and collagen alpha1(I) mRNA in rat pancreatic stellate cells activated by platelet-derived growth factor. *Indian J Gastroenterol* 2005;24:100-103.
28. Anania FA, Womack L, Jiang M, Saxena NK. Aldehydes potentiate alpha2(I) collagen gene activity by JNK in hepatic stellate cells. *Free Radic Biol Med* 2001;30:846-857.
29. Chen A, Davis BH. The DNA binding protein BTEB mediates acetaldehyde-induced, jun N-terminal kinase-dependent alpha1(I) collagen gene expression in rat hepatic stellate cells. *Mol Cell Biol* 2000;20:2818-2826.
30. De Minicis S, Candelaresi C, Marziani M, Saccomano S, Roskams T, Casini A, et al. Role of endogenous opioids in modulating HSC activity in vitro and liver fibrosis *in vivo*. *Gut* 2008;57:352-364.
31. Buttner C, Skupin A, Rieber EP. Transcriptional activation of the type I collagen genes COL1A1 and COL1A2 in fibroblasts by interleukin-4: analysis of the functional collagen promoter sequences. *J Cell Physiol* 2004;198:248-258.
32. Perez de Obanos MP, Lopez-Zabalza MJ, Arriazu E, Modol T, Prieto J, Herraiz MT, Iraburu MJ. Reactive oxygen species (ROS) mediate the effects of leucine on translation regulation and type I collagen production in hepatic stellate cells. *Biochim Biophys Acta* 2007;1773:1681-1688.
33. Comporti M. Three models of free radical-induced cell injury. *Chem Biol Interact* 1989;72:1-56.
34. Fickert P, Thueringer A, Moustafa T, Silbert D, Gumhold J, Tsybrovskyy O, et al. The role of osteopontin and tumor necrosis factor alpha receptor-1 in xenobiotic-induced cholangitis and biliary fibrosis in mice. *Lab Invest* 2010;90:844-852.
35. Chen Y, Bal BS, Gorski JP. Calcium and collagen binding properties of osteopontin, bone sialoprotein, and bone acidic glycoprotein-75 from bone. *J Biol Chem* 1992;267:24871-24878.
36. Singh K, DeVouge MW, Mukherjee BB. Physiological properties and differential glycosylation of phosphorylated and nonphosphorylated forms of osteopontin secreted by normal rat kidney cells. *J Biol Chem* 1990;265:18696-18701.
37. Cho MK, Lee GH, Park EY, Kim SG. Hyaluronic acid inhibits adhesion of hepatic stellate cells in spite of its stimulation of DNA synthesis. *Tissue Cell* 2004;36:293-305.



Author Proof

AQ1: According to editorial policy, abbreviations must be spelled out in titles; therefore, PI3K-pAkt-NFkB has been expanded.

AQ2: Please confirm or correct author names and affiliations.

AQ3: Degrees have been added for corresponding author; please verify as complete and accurate.

AQ4: Please confirm disclosure statement as accurate.

AQ5: Journal style requires only a Conclusion head for Abstract; therefore, Background and Results subheads have been deleted.



**Author Proof**